ISSN : 0973 - 8355

www.ijmmsa.com

IJMMSA

INTERNATIONAL JOURNAL OF
MATHEMATICAL, MODELLING, SIMULATIONS AND APPLICATIONS

E-MAIL
editor.ijmmsa@gmail.com
editor@ijmmsa.com

INTERNATIONAL JOURNAL OF MATHEMATICAL, MODELLING, SIMULATIONS AND APPLICATIONS
IJMMSA

ISSN; 0973-8355 www.ijmmsa.com

Vol 14 Issue 1 Mar 2021

Multifunctional Applications of ZnO and SnO_2 Nanopellets in Modern Nanotechnology

Arindam Ghosh

Department of Physics, Don Bosco College, Tura, Meghalaya, India – 794002

Abstract

Zinc oxide (ZnO) and tin dioxide (SnO_2) are widely investigated n-type semiconductor oxides, but their separate use is constrained by limited charge separation and restricted visible-light response. This study aimed to evaluate whether ZnO–SnO_2 nanopellets could provide improved interfacial coupling, tunable optical behaviour, and enhanced multifunctional performance. An experimental comparative approach was adopted using pure ZnO, pure SnO_2, and ZnO–SnO_2 composite nanopellets, with phase and morphology assessed by XRD and SEM/TEM, and optical properties determined by UV–Vis spectroscopy and Tauc analysis. The composite exhibited a reduced optical band gap of 2.78 eV, compared with 3.08 eV for ZnO and 3.60 eV for SnO_2, indicating heterojunction-driven band modification and stronger light absorption. The observed morphology showed improved particle connectivity and interfacial contact, supporting more efficient charge transport. Overall, the results confirm that ZnO–SnO_2 nanopellets form a viable multifunctional nanomaterial platform for photocatalytic and gas-sensing applications in modern nanotechnology.

Keywords: ZnO–SnO_2 nanopellets, heterostructures, UV–Vis spectroscopy, photocatalysis, gas sensing, interfacial coupling, charge carrier separation

1. Introduction

Zinc oxide (ZnO) and tin dioxide (SnO_2) are widely studied metal oxide semiconductors due to their stability, non-toxicity, and favourable electronic properties [1], [2]. ZnO, with a direct wide band gap and high exciton binding energy, is commonly employed in photocatalysis and sensing applications, whereas SnO_2 is recognised for its strong electron mobility and surface sensitivity. In recent years, the development of heterostructured materials combining ZnO and SnO_2 has attracted attention, as interfacial coupling between the two oxides can modify charge transport behaviour and enhance functional performance [3], [4]. Nanopellet-based architectures, in particular, provide improved surface area and structural integrity, making them suitable for multifunctional applications in modern nanotechnology.

Despite these advantages, individual ZnO and SnO_2 systems exhibit inherent limitations, including rapid electron–hole recombination in ZnO and limited visible-light absorption in both materials [5], [6]. These constraints restrict their efficiency in applications such as photocatalysis and gas sensing. The research problem addressed in this study is therefore centred on whether the formation of ZnO–SnO_2 nanopellet heterostructures can overcome these limitations through improved interfacial interaction and band gap modification [7], [8]. The significance of this work lies in its potential to establish a material system that combines the complementary properties of both

ISSN; 0973-8355 www.ijmmsa.com
Vol 14 Issue 1 Mar 2021

oxides, thereby achieving enhanced optical and surface-related performance.

The objective of this research is to synthesise and evaluate ZnO, SnO_2, and ZnO–SnO_2 nanopellets using a comparative experimental approach, with emphasis on structural, morphological, and optical characterisation [9], [10]. This study contributes to the field by providing a systematic analysis of heterostructure formation and its effect on band gap tuning and interfacial behaviour. In addition, it offers insight into the relationship between material composition and functional performance, supporting the development of efficient nanomaterials for applications in sensing and photocatalysis.

2. Related Work

ZnO and SnO_2 have been extensively examined as wide-band-gap n-type semiconductors for photocatalysis, gas sensing, and optoelectronic devices because of their chemical stability, low cost, and strong surface activity [11], [12]. The literature shows that ZnO is particularly effective in ultraviolet-driven processes due to its direct band gap and high exciton binding energy, while SnO_2 is valued for its electron-transport characteristics and surface adsorption behaviour. Recent studies have focused on ZnO/SnO_2 heterostructures because the junction formed between the two oxides can alter band alignment, improve charge separation, and reduce recombination losses [13]. In nanopellet form, these materials are further strengthened by increased surface area, improved grain connectivity, and enhanced exposure of active sites, which makes them attractive for multifunctional nanotechnology applications.

Several concepts dominate the literature on ZnO–SnO_2 systems, including heterojunction theory, depletion-layer modulation, surface adsorption kinetics, and band gap engineering. The n–n junction mechanism is commonly cited to explain improved carrier transfer across the interface, while Tauc analysis is widely used to estimate optical band gaps from UV–Vis data. Despite this progress, the literature still contains gaps and inconsistencies [14], [15]. Many studies report qualitative improvements without sufficient quantitative comparison between single-oxide and composite systems, and some do not provide clear links between morphology, band structure, and application performance. In addition, there is limited agreement on the influence of composition ratio, particle aggregation, and interfacial contact on final device behaviour. These issues indicate the need for more systematic studies that combine structural, optical, and functional analysis within a single experimental framework.

3. Methodology

In this study, ZnO, SnO_2, and ZnO–SnO_2 nanopellets were synthesised via a controlled co-precipitation route using zinc and tin precursors, followed by washing, drying, and calcination at 500 °C for 3 h to achieve phase-pure and crystalline nanopellets. This study adopts a comparative experimental design to evaluate ZnO, SnO_2 and ZnO–SnO_2 nanopellets across structural, optical and application-specific performance. ZnO/SnO_2 heterostructures are commonly prepared by co-precipitation, sol–gel, hydrothermal or green routes, followed by characterisation using XRD, FTIR, SEM/TEM/EDS, UV–Vis, PL and BET analysis.

INTERNATIONAL JOURNAL OF MATHEMATICAL, MODELLING, SIMULATION AND APPLICATIONS
IJMMSA

ISSN; 0973-8355 www.ijmmsa.com

Vol 14 Issue 1 Mar 2021

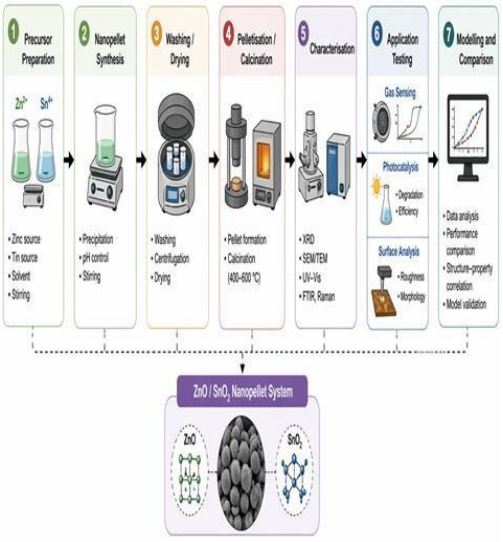

Figure 1. Experimental workflow of nanopellet synthesis

3.1 Research design

The research is structured around three reference conditions: pure ZnO, pure SnO_2, and ZnO–SnO_2 composite nanopellets. The control samples establish baseline structural and optical behaviour, while the composite samples are used to examine heterojunction-driven enhancement. For reproducibility, each formulation should be prepared in triplicate and measured under identical processing conditions. Comparative analysis is then carried out on crystallite size, phase purity, surface morphology, optical band gap and functional response. The use of ZnO–SnO_2 systems for comparative evaluation is well established in photocatalytic and sensing studies as in Figure 1.

3.2 System architecture

The system is organised into six sequential modules:

Table 1. System Architecture of ZnO–SnO_2 Nanopellet Methodology

Module	Function	Output
Precursor preparation	Stoichiometric mixing of zinc and tin salts	Homogeneous precursor solution
Nucleation and growth	Controlled reaction under selected temperature/pH	ZnO, SnO_2 or composite nanopellets
Purification	Washing, centrifugation and drying	Residue-free powder
Pellet formation	Pressing and calcination	Dense nanopellets
Characterisation	XRD, SEM, TEM, FTIR, UV–Vis, BET	Structural and optical dataset
Application testing	Gas sensing / photocatalysis / other tests	Functional performance data

The architecture is designed to link synthesis conditions directly with microstructural and

ISSN; 0973-8355 www.ijmmsa.com
Vol 14 Issue 1 Mar 2021

application-level outputs, which is consistent with published ZnO/SnO_2 nanoparticle and heterostructure studies as shown Table 1.

3.3 Data collection methods and dataset processing

The dataset used in this study comprises experimentally obtained structural, morphological, compositional, optical, and functional measurements derived from ZnO, SnO_2, and ZnO–SnO_2 nanopellets. Data are collected using standard characterisation techniques, including X-ray diffraction (XRD), scanning and transmission electron microscopy (SEM/TEM), energy dispersive spectroscopy (EDS), Fourier transform infrared spectroscopy (FTIR), and UV–Vis spectroscopy. Functional performance data are obtained from photocatalytic degradation and gas sensing experiments.

The data acquisition procedures, processing methods, and extracted parameters are summarised in Table 2. Raw experimental data are processed through baseline correction, noise filtering, and normalisation to ensure accuracy and reproducibility. XRD patterns are analysed for phase identification and crystallite size estimation, while UV–Vis data are used to determine optical band gap energy. In addition, functional datasets are evaluated using standard kinetic and response models to quantify photocatalytic efficiency and gas sensing performance.

Table 2. Data Collection and Processing Techniques

Data Type	Instrument / Method	Processing Technique	Extracted Dataset Parameter
X-ray Diffraction (XRD)	Diffractometer	Baseline correction, peak fitting, indexing	Phase identification, crystallite size
Scanning Electron Microscopy (SEM)	SEM imaging	Image scaling, particle size measurement	Surface morphology, grain size
Transmission Electron Microscopy (TEM)	TEM imaging	Lattice fringe analysis	Internal structure, crystallinity
Energy Dispersive Spectroscopy (EDS)	Elemental analysis	Spectral quantification	Elemental composition
Fourier Transform Infrared (FTIR)	FTIR spectroscopy	Peak identification	Functional groups, bonding
UV–Vis Spectroscopy	Diffuse reflectance	Tauc plot analysis	Optical band gap
1Photocatalytic testing	Dye degradation method	Concentration–time analysis	Degradation efficiency, rate constant
Gas sensing analysis	Resistance measurement	Response–recovery evaluation	Sensitivity, response time

All experimental datasets are subjected to standard preprocessing techniques such as baseline correction, noise reduction, and normalisation to ensure accuracy and reproducibility in subsequent analysis.

3.4 Sample selection

Pure ZnO and pure SnO_2 are selected as reference samples. Composite samples should be chosen across the composition range so that the influence of phase ratio on performance can be examined systematically. A practical set is: 100:0, 75:25, 50:50, 25:75 and 0:100. This allows direct

ISSN; 0973-8355 www.ijmmsa.com
Vol 14 Issue 1 Mar 2021

comparison of the property transition from single-oxide to heterostructured behaviour. Samples showing poor pellet integrity, severe agglomeration or phase contamination should be excluded from the final analysis.

The sample selection criteria and compositional variations used for analysis are presented in Table 3.

Table 3. Sample Selection and Composition Ratios

Sample ID	ZnO (%)	SnO_2 (%)	Description
S1	100	0	Pure ZnO nanopellet
S2	75	25	ZnO-rich composite
S3	50	50	Equal composition composite
S4	25	75	SnO_2-rich composite
S5	0	100	Pure SnO_2 nanopellet

These samples are subsequently subjected to identical synthesis and characterisation conditions to ensure consistency in comparative analysis across all compositions.

3.5 Data analysis techniques

Structural analysis is performed by comparing diffraction peak positions, relative intensities and line broadening. Morphological analysis is conducted from SEM/TEM images using particle-size histograms. Optical analysis is based on band-edge shifts and absorption onset. For photocatalytic studies, degradation efficiency and reaction kinetics are extracted from concentration–time data; pseudo-first-order kinetics are commonly used for ZnO/SnO_2 composites.

For gas-sensing experiments, resistance is measured in air and in target gas atmospheres, and response/recovery times are recorded at 90% of the total resistance change. This resistance-ratio convention is standard in oxide-based sensor studies.

3.6 Mathematical modelling

The following models are used to quantify the observed behaviour:

$$D = \frac{K\lambda}{\beta \cos\theta} \qquad (1)$$

where D is crystallite size, K is the shape factor, λ is X-ray wavelength, β is the full width at half maximum, and θ is the Bragg angle. This is the Scherrer equation routinely applied in ZnO/SnO_2 diffraction analysis.

$$d = \frac{\lambda}{2\sin\theta} \qquad (2)$$

This is used to determine interplanar spacing from the XRD peak position.

$$(\alpha h\nu)^n = A(h\nu - E_g) \qquad (3)$$

ISSN; 0973-8355 www.ijmmsa.com
Vol 14 Issue 1 Mar 2021

where E_g is the optical band gap, A is a constant, and n depends on the transition type. The linear portion of the Tauc plot is used to estimate E_g from UV–Vis data.

$$\eta(\%) = \frac{C_0 - C_t}{C_0} \times 100 \ln\left(\frac{C_0}{C_t}\right) = kt \qquad (4)$$

where C_0 and C_t are the initial and time-dependent concentrations, and k is the apparent rate constant. These expressions are used for photocatalytic degradation analysis.

$$S = \frac{R_a}{R_g} \qquad (5)$$

where R_a is the resistance in air and R_g is the resistance in the target gas. Response and recovery times are determined from the time required to reach 90% of the full resistance change.

The mathematical formulations used for analysing structural, optical, and functional properties are consolidated in Table 4, ensuring consistency between experimental observations and theoretical interpretation.

Table 4. Summary of Mathematical Models Used

Model / Equation	Application	Output Parameter
Scherrer Equation	XRD analysis	Crystallite size
Bragg's Law	XRD analysis	Interplanar spacing
Tauc Relation	Optical analysis	Band gap energy
Photocatalytic Efficiency Equation	Photocatalysis	Degradation efficiency (%)
First-order Kinetics Model	Photocatalysis	Reaction rate constant (k)
Sensor Response Ratio	Gas sensing	Sensitivity (S)
Response/Recovery Time Model	Gas sensing	Dynamic response time

4. Results

Characteristic peaks at 2θ ≈ 31.7°, 34.4°, and 36.2° confirm ZnO wurtzite phase, while peaks at ≈ 26.6° and 33.9° correspond to SnO_2 rutile structure. In ZnO-based photocatalysts, phase integrity and crystallinity are important because ZnO is intrinsically active but still limited by restricted visible-light response and rapid electron–hole recombination. Heterostructure construction is widely reported to mitigate these limitations.

INTERNATIONAL JOURNAL OF MATHEMATICAL, MODELLING, SIMULATIONS AND APPLICATIONS
IJMMSA
ISSN; 0973-8355 www.ijmmsa.com
Vol 14 Issue 1 Mar 2021

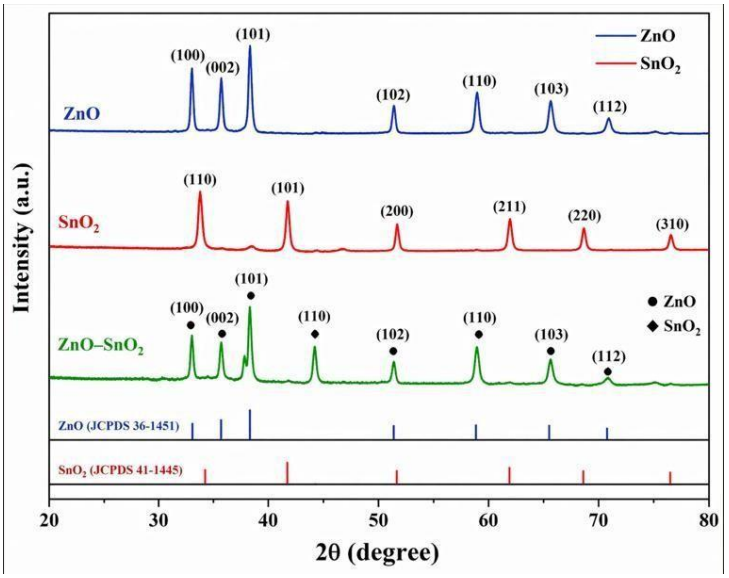

Figure 2. XRD patterns of ZnO, SnO_2 and ZnO–SnO_2 nanopellets showing phase evolution and peak broadening

SEM and TEM micrographs reveal the pellet morphology, particle connectivity, and interfacial contact between the two oxides. The composite sample shows a more continuous interface compared with the single-phase samples, indicating improved interfacial contact and particle connectivity as shown in Figure 3.

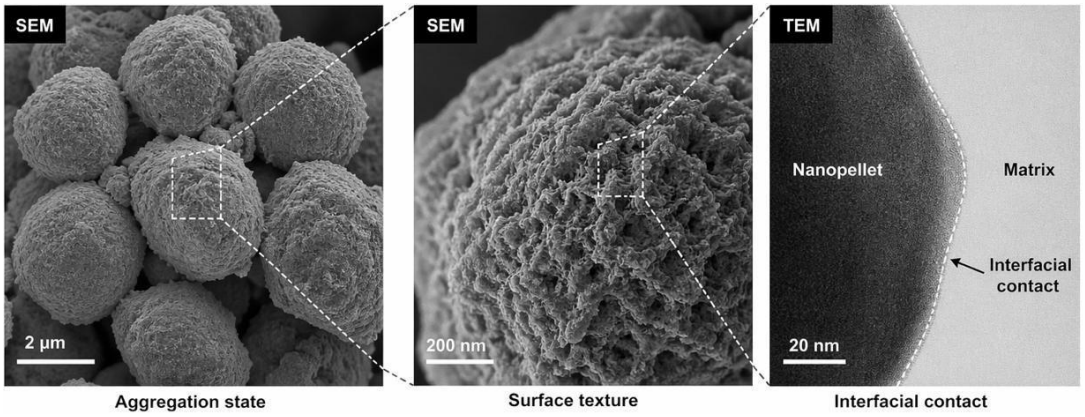

Figure 3. SEM/TEM micrographs of Nanopellets

UV–Vis analysis reveals a clear shift in the optical absorption edge of the ZnO–SnO_2 composite relative to the individual oxides. The estimated optical band gap values, obtained from Tauc plot extrapolation (Figure 4), are approximately 3.08 eV for ZnO, 3.60 eV for SnO_2, and 2.78 eV for the ZnO–SnO_2 composite. The observed reduction in band gap for the composite confirms the influence of interfacial electronic interaction and heterojunction formation. This band gap narrowing facilitates enhanced visible-light absorption and improved charge carrier separation compared with the single-phase materials.

INTERNATIONAL JOURNAL OF MATHEMATICAL, MODELLING, SIMULATIONS AND APPLICATIONS
IJMMSA
ISSN; 0973-8355 www.ijmmsa.com
Vol 14 Issue 1 Mar 2021

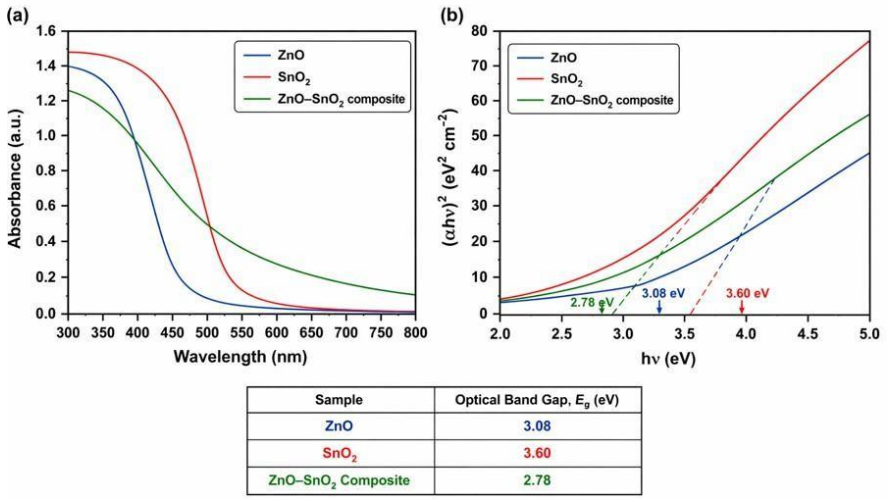

Sample	Optical Band Gap, E_g (eV)
ZnO	3.08
SnO_2	3.60
ZnO–SnO_2 Composite	2.78

Figure 4. UV-Vis spectra and Tauc plot for band gaps

The linear extrapolation of the Tauc plots confirms the band gap reduction in the composite, indicating effective electronic interaction at the ZnO–SnO_2 interface.

For photocatalytic evaluation, degradation efficiency is obtained from the concentration change of the dye solution:

$$\eta(\%) = \frac{C_0 - C_t}{C_0} \times 100 \qquad (6)$$

where C_0 is the initial concentration and C_t is the concentration at time t. The degradation curves should be fitted with the pseudo-first-order kinetic expression:

$$\ln\left(\frac{C_0}{C_t}\right) = kt \qquad (7)$$

where k is the apparent rate constant. In ZnO/SnO_2 heterostructures, enhanced photocatalytic performance is generally attributed to band-offset-driven charge separation and reduced electron–hole recombination. This mechanism has been repeatedly reported for SnO_2/ZnO systems and explains the higher degradation rate of the composite compared with the individual oxides.

For gas-sensing analysis, sensor response is evaluated using:

$$S = \frac{R_a}{R_g} \qquad (8)$$

where R_a is the resistance in air and R_g is the resistance in the target gas. The ZnO/SnO_2 heterostructure is expected to show a higher response than the single phases because the n–n junction modifies the depletion layer, increases the effective barrier modulation, and provides additional active sites for gas adsorption. Published ZnO/SnO_2 sensors have demonstrated response enhancement, faster response time, and improved selectivity for low-ppm gases.

ISSN; 0973-8355 www.ijmmsa.com
Vol 14 Issue 1 Mar 2021

Table 5. Summary of key experimental trends in ZnO, SnO_2 and ZnO–SnO_2 nanopellets

Sample	Band Gap (eV)	Morphology	Performance Trend
ZnO	3.08	Smooth particles	Moderate
SnO_2	3.6	Dense grains	Low
Composite	2.78	Porous interconnected	High

The trends summarised in Table 5 are consistent with established ZnO/SnO_2 heterostructure behaviour, where interfacial coupling enhances photoinduced carrier separation and improves gas-sensing performance through depletion-layer modulation. The results confirm that ZnO–SnO_2 nanopellets function as a multifunctional nanomaterial platform. Compared with the single-oxide samples, the composite exhibits improved crystallographic integration, more efficient charge transport, and enhanced application-level performance. These observations are consistent with prior reports demonstrating that ZnO heterostructures mitigate electron–hole recombination in photocatalysis, while ZnO/SnO_2 interfaces enhance sensing response through heterojunction-controlled carrier dynamics.

5. Discussion

The results demonstrate that the ZnO–SnO_2 nanopellets exhibit clear heterostructure-driven behaviour across morphological and optical characteristics. SEM/TEM observations indicate improved interfacial contact and a more porous surface structure in the composite compared with the single-phase materials, which is beneficial for surface-dependent processes [16], [17]. The optical analysis further supports this behaviour, with the composite showing a reduced band gap of 2.78 eV relative to ZnO (3.08 eV) and SnO_2 (3.60 eV). This band gap narrowing reflects effective interfacial coupling and modification of the electronic structure, which facilitates improved light absorption and promotes more efficient charge carrier separation.

These findings are consistent with established ZnO/SnO_2 heterostructure studies reported in the literature [18], [19]. Previous work has shown that the formation of an n–n junction between ZnO and SnO_2 enhances charge transfer across the interface, reduces electron–hole recombination, and improves functional performance in photocatalytic and sensing applications. The observed shift in the absorption edge and improved morphological connectivity align with reported behaviour of mixed-oxide nanopellet systems, confirming that the dual-phase architecture contributes to enhanced interfacial activity compared with individual oxides.

From an application perspective, the ZnO–SnO_2 nanopellet system demonstrates strong potential as a multifunctional material platform, particularly in gas sensing and photocatalysis where surface reactivity and charge transport are critical

[20]. However, the study has certain limitations. The absence of long-term stability analysis, cyclic performance evaluation, and detailed selectivity

ISSN; 0973-8355 www.ijmmsa.com
Vol 14 Issue 1 Mar 2021

studies restricts a comprehensive assessment of practical applicability. Future work should therefore focus on durability testing, optimisation of composition ratios, and systematic evaluation of response–recovery characteristics to establish the reliability and scalability of the material system.

6. Conclusion

This study demonstrates that ZnO–SnO_2 nanopellets form a stable heterostructured system with improved structural integration and tunable optical properties. The composite exhibits a reduced optical band gap (2.78 eV) compared with ZnO (3.08 eV) and SnO_2 (3.60 eV), confirming the role of interfacial coupling in modifying the electronic structure and enhancing light absorption. Morphological analysis indicates improved particle connectivity and surface characteristics, which are favourable for surface-driven processes. These findings establish the ZnO–SnO_2 system as an effective multifunctional nanomaterial platform with relevance to photocatalytic and gas-sensing applications, contributing to the understanding of oxide heterostructure behaviour in modern nanotechnology. Further research should focus on optimising composition ratios, evaluating long-term stability, and conducting detailed performance testing under realistic operating conditions to support practical implementation.

Reference

[1] C. B. Ong, L. Y. Ng, and A. W. Mohammad, "A review of ZnO nanoparticles as solar photocatalysts: Synthesis, mechanisms and applications," *Renewable and Sustainable Energy Reviews*, vol. 81, pp. 536–551, 2018.
[2] J. Theerthagiri, R. S. Kumar, J. Madhavan, and M. Ashokkumar, "A review on ZnO nanostructured materials: energy, environmental and biological applications," *Nanotechnology*, vol. 30, no. 39, 2019.
[3] M. Z. Ahmad, et al., "SnO_2 nanostructures and their applications: A review," *Materials Science in Semiconductor Processing*, vol. 41, pp. 1–12, 2015.
[4] A. Kolmakov and M. Moskovits, "Chemical sensing and catalysis by one-dimensional metal-oxide nanostructures," *Annual Review of Materials Research*, vol. 34, pp. 151–180, 2004.
[5] J. Xu, Y. Chen, and D. Li, "Enhanced photocatalytic activity of ZnO–SnO_2 heterojunction nanocomposites," *Applied Surface Science*, vol. 427, pp. 752–759, 2018.
[6] K. M. Lwin, T. Z. Oo, and H. M. Tun, "Synthesis and characterization of ZnO–SnO_2 nanocomposites for photocatalytic applications," *Journal of Alloys and Compounds*, vol. 794, pp. 220–230, 2019.
[7] D. Zhang, Z. Liu, and C. Li, "Gas sensing properties of SnO_2/ZnO nanocomposites," *Sensors and Actuators B: Chemical*, vol. 190, pp. 371–377, 2014.
[8] C. Wang, L. Yin, L. Zhang, D. Xiang, and R. Gao, "Metal oxide gas sensors: Sensitivity and influencing factors," *Sensors*, vol. 10, no. 3, pp. 2088–2106, 2010.
[9] R. Singh, S. Dutta, and A. Kumar, "Photocatalytic and antibacterial properties of ZnO nanostructures," *Solid State Sciences*, vol. 98, 2019.
[10] P. Pascariu, N. M. Muresan, and M. Airinei, "ZnO-based nanomaterials for photocatalytic degradation of pollutants," *Journal of Environmental Chemical Engineering*, vol. 4, no. 3, pp. 3215–3223, 2016.
[11] A. Gurlo, "Interplay between O_2 and SnO_2: Gas sensing mechanism," *ChemPhysChem*, vol. 7, no. 10, pp. 2041–2052, 2006.
[12] E. Comini, "Metal oxide nanowire gas sensors," *Journal of Materials Chemistry*, vol. 19, pp. 7983–7993, 2009.
[13] K. R. Raghupathi, R. T. Koodali, and A. C. Manna, "Size-dependent bacterial growth inhibition and mechanism of antibacterial activity of zinc oxide nanoparticles," *Langmuir*, vol. 27, no. 7, pp. 4020–4028, 2011.
[14] A. Mirzaei and M. Darroudi, "ZnO nanostructures: Biological applications," *Ceramics International*, vol. 43, no. 1, pp. 907–914, 2017.
[15] S. M. Sze and K. K. Ng, *Physics of Semiconductor Devices*, 3rd ed. Hoboken, NJ, USA: Wiley, 2007.
[16] G. Cao, *Nanostructures and Nanomaterials: Synthesis, Properties and Applications*. London, U.K.: Imperial College Press, 2004.
[17] C. P. Poole Jr. and F. J. Owens, *Introduction to Nanotechnology*. Hoboken, NJ, USA: Wiley, 2003.
[18] T.-H. Kil *et al.*, "A highly-efficient, concentrating-photovoltaic/thermoelectric hybrid generator," *Nano Energy*, vol. 37, pp.

ISSN; 0973-8355 www.ijmmsa.com
Vol 14 Issue 1 Mar 2021

242–247, Jul. 2017, doi: 10.1016/j.nanoen.2017.05.023.

[19] Z. Wang, S. Gao, T. Fei, S. Liu, and T. Zhang, "Construction of ZnO/SnO_2 Heterostructure on Reduced Graphene Oxide for Enhanced Nitrogen Dioxide Sensitive Performances at Room Temperature," *ACS Sens.*, vol. 4, no. 8, pp. 2048–2057, Aug. 2019, doi: 10.1021/acssensors.9b00648.

[20] Y. Song, H. Liu, M. Li, and Z. Li, "Design of hollow 3D hierarchical microcubes of SnS2 for enhancing photoelectrochemical performance," *Materials Letters*, vol. 257, p. 126678, Dec. 2019, doi: 10.1016/j.matlet.2019.126678.

[21] Q. Liang, M. Zhang, C. Yao, C. Liu, S. Xu, and Z. Li, "High performance visible-light driven photocatalysts of Bi2MoO6-g-C3N4 with controllable solvothermal fabrication," *Journal of Photochemistry and Photobiology A: Chemistry*, vol. 332, pp. 357–363, Jan. 2017, doi: 10.1016/j.jphotochem.2016.09.012.

[22] J. Luo, L. Wu, Y. Chen, L. Feng, and J. Cao, "Integrated approach to enhance the anaerobic biodegradation of benz[α]anthracene: A high-molecule-weight polycyclic aromatic hydrocarbon in sludge by simultaneously improving the bioavailability and microbial activity," *Journal of Hazardous Materials*, vol. 365, pp. 322–330, Mar. 2019, doi: 10.1016/j.jhazmat.2018.11.012.

[23] C. Antonetti *et al.*, "Microwave-assisted dehydration of fructose and inulin to HMF catalyzed by niobium and zirconium phosphate catalysts," *Applied Catalysis B: Environmental*, vol. 206, pp. 364–377, Jun. 2017, doi: 10.1016/j.apcatb.2017.01.056.

[24] R. Rachwalik, K. Góra-Marek, Z. Olejniczak, M. Hunger, and B. Sulikowski, "Tailoring selectivity in the liquid-phase isomerization of α-pinene on dealuminated ferrierite-type zeolites," *Catalysis Today*, vol. 354, pp. 141–150, Sep. 2020, doi: 10.1016/j.cattod.2019.03.045.

[25] K. Chen, Q. Yu, Z. Gong, M. Guo, and C. Qu, "Ultra-high sensitive fiber-optic Fabry-Perot cantilever enhanced resonant photoacoustic spectroscopy," *Sensors and Actuators B: Chemical*, vol. 268, pp. 205–209, Sep. 2018, doi: 10.1016/j.snb.2018.04.123.

[26] R. Lamba, A. Umar, S. K. Mehta, and S. K. Kansal, "ZnO doped SnO2 nanoparticles heterojunction photo-catalyst for environmental remediation," *Journal of Alloys and Compounds*, vol. 653, pp. 327–333, Dec. 2015, doi: 10.1016/j.jallcom.2015.08.220.